Supplemental Methods

Mouse Studies: Mouse studies were approved by Northwestern's Animal Care and Use Committee. *GM3 synthase* knockout ($GM3S^{-/-}$) mice (Yamashita *et al.*, 2003) (courtesy of Dr. R. Proia, NIH; C57BL/6-129/svev background) were backcrossed a total of 13 times to C57BL/6 mice (Jackson Laboratory, Bar Harbor, MA) to produce fully congenic $GM3S^{-/-}$ mice and their wildtype littermate controls ($GM3S^{+/+}$, WT). Mice were fed either a regular diet (RD) containing 11.4% fat, 62.8% carbohydrate, and 25.8% protein (total 12.6 kJ/g, Harlan Teklad 7012, Indianapolis, IN) or a high fat diet (HFD) consisting of 42% fat, 25.6% carbohydrate, and 16.4% protein (total 23.4 kJ/g, Harlan Teklad TD88137, IN).

Glucose tolerance testing and insulin measurements. Mice were fasted overnight before injecting intraperitoneally with D-glucose (2 g/kg). Blood was obtained by tail nick at baseline, 30, 60, and 120 min after glucose administration (Yamashita *et al.*, 2003). For measuring insulin, whole blood obtained from the intraorbital retrobulbar plexus was allowed to clot at RT for 30 min before centrifugation at 4°C to separate serum from clotted blood component, and serum was stored at -80°C until insulin was measured using Ultra Sensitive Mouse Insulin ELISA Kit (Crystal Chem Inc., Downers Grove, IL). Absorbance was read at 450 nm in an EL808 microplate reader (BIO-TEK Inc., Winooski, VT) linked with the KC Junior program.

Wound healing. The dorsal surface of mice was shaved, depilated, and wounded 24 h later (Galiano *et al.*, 2004). 5 mm wounds were made with a punch biopsy on each side of the midline to the level of the panniculus carnosus. A donut-shaped silicone splint with a 10 mm outer diameter and a 6 mm inner diameter was centered on the wound and fixed to the skin using a

medical grade liquid contact adhesive (No Tape Liquid Adhesive, Vapon Inc., Fairfield, NJ) and interrupted 6-0 nylon sutures (Ethicon Inc., Somerville, NJ). A semiocclusive dressing (Tegaderm, 3M, St. Paul, MN) was then applied to the wound over a nonstick (Telfa) pad to prevent epidermal disruption. Wound closure was analyzed by tracing the wound margin and calculating the pixel area using digital imaging (Axiovision version 4.5) of photographs taken at 5 cm from the mouse. The non-healed wound area was calculated as the percent open area of the original wound area. Because the splint has a constant area, it served as a visual cue to the initial size of the wound. Wound closure was analyzed at days 3, 5, 7, and every 3 days until healed by tracing the wound margin and calculating the pixel area using digital imaging (Axiovision version 4.5) of photographs taken at 5 cm from the mouse. The non-healed wound area was calculated as the percent open area of the original wound area. Because the splint has a constant area, it served as a visual cue to the initial size of the wound. At termination, the entire wound was harvested for histologic and RNA expression studies with a 10 mm punch biopsy centered in the wound.

Histological studies. Harvested wounds were paraffin-embedded for routine histological and immunohistochemical analyses (Repertinger *et al.*, 2004; Shirakata *et al.*, 2005). Stained 4 μm sections were photographed at 10X magnification under light microscopy (Zeiss Axioplan 2 imaging, Thornwood, NY), and imaged digitally (Axiovision version 4.5) to measure the epidermal gap and area of granulation tissue. The epidermal gap was defined as the maximal gap between the leading edges of epidermal migration, with an epidermal gap of 0 μm representing a completely re-epithelialized wound. The area of granulation tissue was calculated by tracing regions of granulation tissue, calculating pixel area, and adding the areas of these regions. At

least 20 wound specimens per group were analyzed at each time point. For bromodeoxyuridine (BrdU) incorporation testing in 3-day wounds, mice were injected intraperitoneally with BrdU (2g/kg) 2 h before sacrifice. Labeling was detected immunohistochemically with anti-BrdU antibody (Developmental Studies Hybridoma Bank, Iowa City, IA). Using AxioVision computer-assisted morphometric software (Carl Zeiss), the percentage of basal KCs with BrdU-labeled nuclei was determined in the proliferating segment, as defined by the first labeled KC proximal to the wound margin to a labeling index of less than 10% of KCs. KC migration across the wound was quantified as the length along the basement membrane of basal epidermis from the wound edge to the first BrdU-labeled KC. Cells were counted by two pre-trained blinded observers. Sections from at least 20 wounds per group were assessed in each set for BrdU staining.

Reverse Transcription, Droplet Digital PCR and Real-Time PCR. Total RNA was isolated from skin using Trizol reagent (Invitrogen) or from cultured cells using an RNeasy Mini Kit (Qiagen, Valencia, CA) per manufacturers' instructions. One μg of total RNA was reverse transcribed using qScript cDNA Supermix (Quanta Biosciences, Houston, TE) according to manufacturer's instructions. Three μL of diluted (1:5) cDNA product was used for each qRT-PCR reaction using PerfeCTa SYBR Green Supermix with ROX (Quanta Biosciences) to determine the gene expression of GM3S, IR, IGF-1R, and IRS-1 (Wei *et al.*, 2011). Samples were run in triplicate using an ABI Prism 7000 (Applied Biosystems, Carlsbad, CA) for 40 cycles (95ºC for 15 s and 60ºC for 1 min) after an initial incubation at 50ºC for 2 min and 95ºC for 10 min. Amplification specificity was checked by both melting curve analysis and gel electrophoresis. The fold change in expression of each gene was calculated using the $\Delta\Delta C_t$ method with GAPDH as the internal

control for normalization. Droplet digital PCR (ddPCR) was performed on QX100 PCR system (Bio-Rad, Hercules, CA). Each ddPCR reaction mixture contains 5 ng of template, 2X ddPCR Mastermix, 20X primer, and probes (final concentrations of 900 and 250 nM, respectively) in a final volume of 20 μL. Each mixture was loaded into the sample well of DG8 cartridge (Bio-Rad) and a volume of 70 μL of droplet mineral oil (Bio-Rad) was added into each sample. The cartridge was placed into the droplet generator (Bio-Rad) for emulsification before transferring into a 96-well PCR plate. The plate was heat-sealed and placed on a thermal cycler (Bio-Rad) and amplified for 40 cycles. The 96-well PCR plate was then loaded on the droplet reader (Bio-Rad), which automatically reads the droplets. Analysis of the ddPCR data was performed with QuantaSoft analysis software (Bio-Rad). Primer sequences are listed in Supplemental Table 1.

Proliferation and scratch assays. For proliferation assays, KCs were plated onto 96-well ($2x10^3$ cell/well) or 12-well ($2x10^4$ cell/well) plates and cell proliferation was assessed daily for 5 d by both Water Soluble Tetrazolium assay (96-well plate) per manufacturer's instruction (Clontech, Mountain View, CA) and manual counting using a hemacytometer (12-well plate). For scratch assays, confluent monolayer KCs were treated with high Ca^{2+} (1mM) containing CnT-07 complete medium for 4 h to force cells to move as a sheet, and 5 μg/mL mitomycin was added to prevent proliferation one hour before the scratch was made with a 10 μL pipette tip. Cell migration in complete high Ca^{2+} containing CnT-07 medium in the presence of 4 μg/mL mitomycin was recorded photographically every 12 h for 60 h under an inverted phase-contrast microscope (Nikon, Japan). The unfilled scratch area was measured using AxioVision software and recorded as the total pixels of the open area. The ratio of total pixels of filled area/total pixels of initial unfilled (scratched) area among various groups was compared at each time point.

For studies with inhibitors, pretreated cells were plated onto 96-well plate (for proliferation assay) or 12-well plates (for scratch migration assay) and cells were allowed to attach for 4 h before purified LacCer, GM3, glucose, AG538, or LY294002 was added back into each corresponding well (and replenished daily). In preliminary studies, antibody directed against IR recognized multiple bands and was toxic to KCs at concentrations that inhibited IR. As a result, IR was knocked down with IR shRNA (Santa Cruz) to study IR function.

Immunoblotting, Immunoprecipitation and In-Cell ELISA. Total protein from whole cell lysate was harvested in RIPA buffer. Monoclonal antibody directed against p-IR was from Millipore (Billevica, MA), and secondary antibodies were from Jackson ImmunoResearch Labs (West Grove, PA); anti-IR, anti-IGF-1R, anti-p-IGF-1R, anti-GM3S, and anti-IRS-1 were polyclonal antibodies from Santa Cruz (Santa Cruz, CA); anti-p-IRS-1 monoclonal antibody, PY-20, anti-Akt, and anti-Akt-p-serine473 were from Cell Signaling Technology (Panvers, MA). GAPDH expression was probed with anti-GAPDH antibody (Santa Cruz) as a loading control. Band density was assessed using the NIH ImageJ program and differences in receptor phosphorylation among groups were compared after normalization based on its GAPDH band density. In-Cell ELISA was performed using In-Cell ELISA Colorimetric Detection Kit per manufacturer's instruction (Pierce, Rockford, IL). In brief, pretreated cells (10,000 cells/well) were plated into 96-well plate overnight before cells were fixed (4% formaldehyde for 15 mins), permeabilized (permeabilization buffer for 15 mins), and blocked (Blocking Buffer for 30 mins). The relative amount of target molecules was determined using target-specific primary antibodies and a horseradish peroxidase (HRP)-conjugated detection reagent, followed by colorimetric measurement of HRP activity at 450 nm to determine absorbance (EL808 microplate reader,

BIO-TEK Inc.). Cells in each well were stained with Janus Green to determine cell number per well. Results were analyzed by normalizing absorbance (HRP activity) values to cell number to adjust for the cell plating differences.

Immunofluorescent staining. To detect GM3 expression, cells plated onto glass slides were treated as described in complete medium for 3 days. After starvation of glucose and growth factors overnight, cells were stimulated with or without insulin (5 μg/mL, 15 mins) or IGF-1 (100 ng/mL, 30 mins) before fixation in cold 4% methanol-free paraformaldehyde for 10 mins. Cells were blocked and permeabilized with 1% BSA/10% goat serum/0.3 M glycine in 0.1% PBS-Tween 20 for 1 h, followed by incubation with anti-GM3 (Seikagaku Corp., Japan) overnight at 4°C. FITC-conjugated anti-mouse IgG was used to detect the expression of GM3 with 10 mM 4′,6-diamidino-2-phenylindole (DAPI) counterstaining. Images were captured using the Nikon A1R (Nikon, Japan) confocal imaging system.

Supplemental Table 1. Primers for qRT-PCR

Primer Name	Gene Name	Sequences (5'- 3')	Product Size (BP)
Human GM3S	St3gal5	/56FAM/CTCTCCTCT/ ZEN/GCATCAGCCTCATCAG/3IABkFQ/ Forward: CTGCCTTTGACATCCTTCAGT Reverse: CATATCCAAAACCCGCCAAAC	140
Mouse GM3S	St3gal5	Qiagen Quantitect Primer Assay, Catalog No. QT02254280	123
Mouse IR	Insr	Forward: ATCAGGTTCCGAACAGTTGC Reverse: TGTCATCAATGGGCAGTTTG	145
Mouse IGFR-1	Igf1r	Forward: CAGCACTCGTTGTTCTCGGT Reverse: AGCCCATGTGTGAGAAGACC	127
Mouse IRS-1	Irs1	Forward: GCCAGAGGATCGTCAATAGC Reverse: AGACGTGAGGTCCTGGTTGT	135

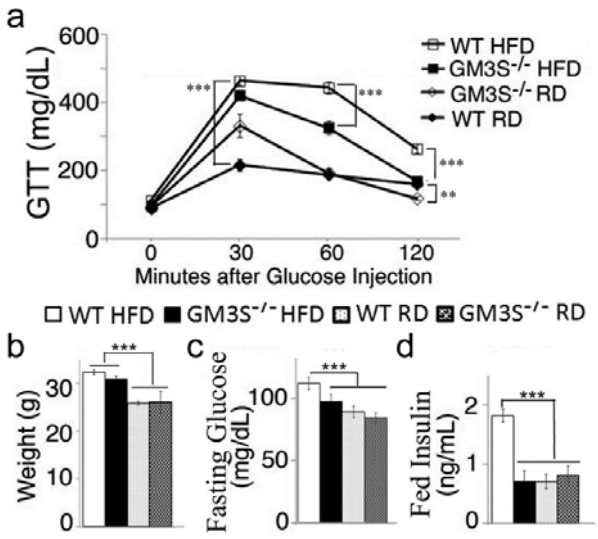

Supplemental Figure 1. **GM3S knockout partially corrects glucose tolerance, but does not reduce fasting glucose or obesity**. (**a**) Glucose tolerance testing in WT and GM3S$^{-/-}$ mice. After overnight fasting, mice were injected i.p. with glucose (2g/kg). (**b**) Mouse weights after 10 wks on HFD or RD. (**c**) Fasting blood glucose. (**d**) Fed insulin. *p<0.05, **p<0.01, ***p<0.001. Data shown as mean ± S.E. n $\geq$ 20 mice per group.

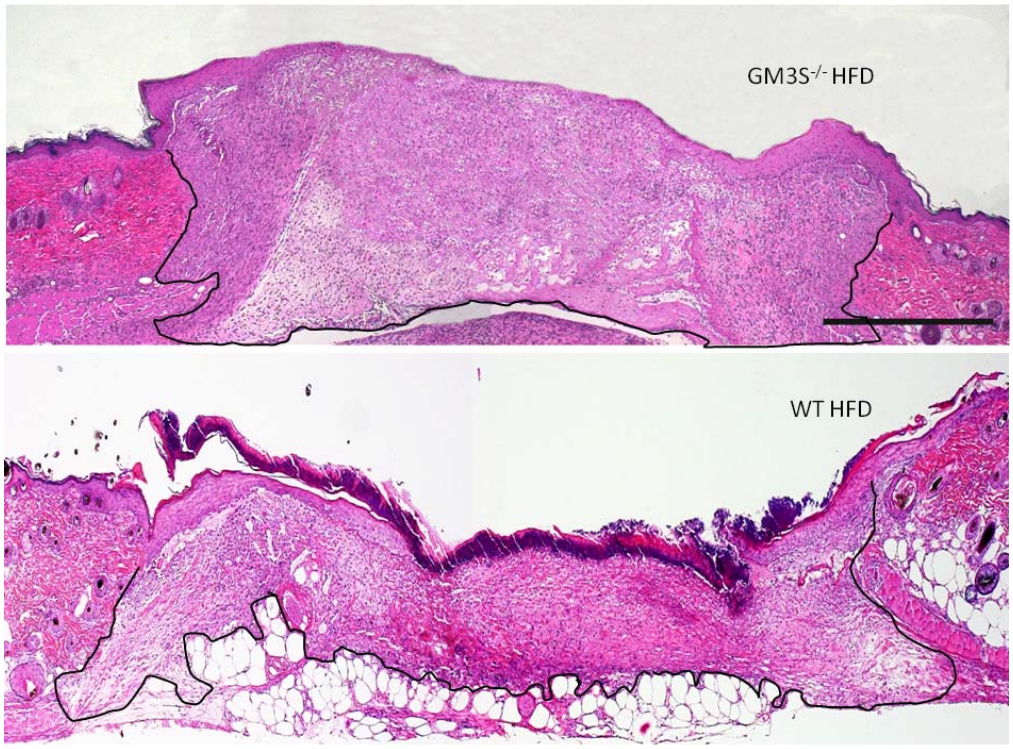

Supplemental Figure 2. **Increased granulation tissue with GM3 depletion**. Granulation tissue is outlined in these 5 day GM3S$^{-/-}$ HFD (upper) vs. WT HFD (lower) mouse wounds. Bar = 400 μm. Granulation tissue measures were performed on at least 20 mice in each group and are shown graphically in Figure 2d.

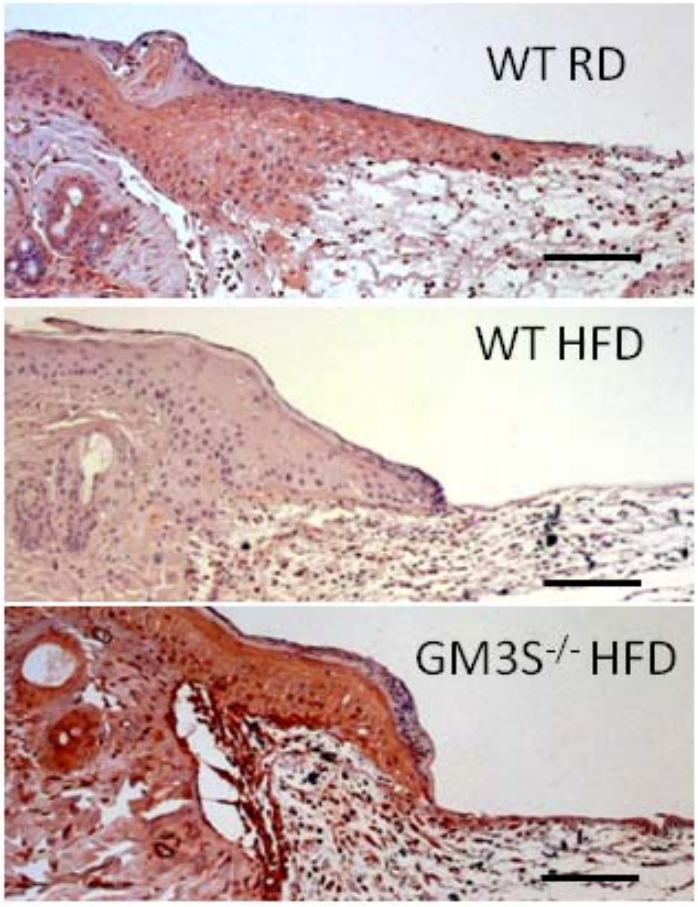

Supplemental Figure 3. **GM3 depletion reverses the suppression of IGF-1R activation the wound skin of DIO mice.** Phosphorylation of IGF-1R in wounds was detected with rabbit polyclonal anti-p-IGF-1R antibody (Santa Cruz) using a Vectastain ABC kit and Nova Red chromogen. Bar = 100 μm. Studies are representative of staining in wounds from at least 4 different mice of each group.

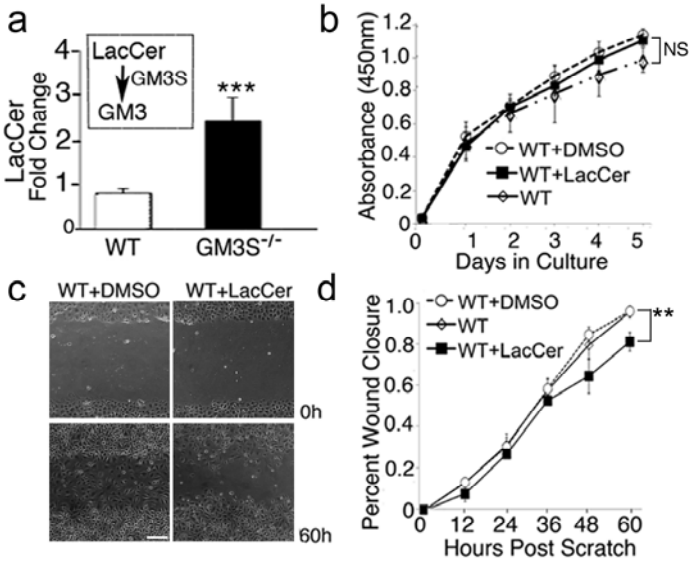

Supplemental Figure 4. **Lactosylceramide does not increase KC migration or proliferation**. (**a**) LacCer expression in WT and GM3S$^{-/-}$ cells was determined by In-Cell ELISA. Inset, schematic of GM3 synthesis from lactosylceramide. ***p<0.001. (**b**) Proliferation of cells treated with and without LacCer or vehicle was examined by water soluble tetrazolium assay. NS = not significant. (**c**) Scratch assays of WT KCs cultured in the presence of 5 μM LacCer or 0.1% DMSO vehicle for 60 hrs. Bar = 50 μm. (**d**) Quantification of wound closure in scratch assays.**p<0.01.

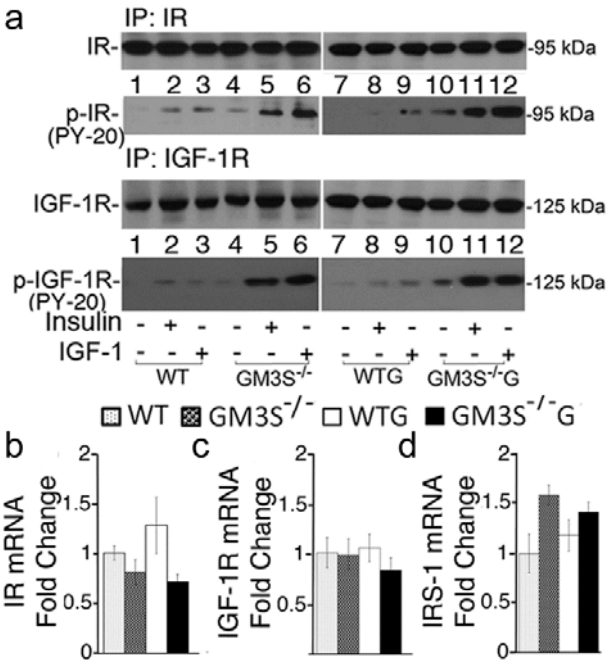

Supplemental Figure 5. **GM3 depletion increases IR and IGF-1R phosphorylation, but not expression of IR, IGF-1R or IRS-1**. (**a**) After WT or GM3S$^{-/-}$ KCs were starved overnight and stimulated with or without insulin or IGF-1, IR and IGF-1R were immunoprecipitated, and phosphorylation of each immunoprecipitated receptor was detected with PY-20 antibody (2nd and 4th rows). Blots were performed 4 times. The expression of IR (**b**), IGF-1R (**c**) and IRS-1 (**d**) was examined by qRT-PCR. No statistically significant differences in expression were found. Primers and reaction conditions for qRT-PCR are presented in Supplemental Table 1 and Supplemental Methods. qRT-PCR was performed 3 times with triplicates for each run.

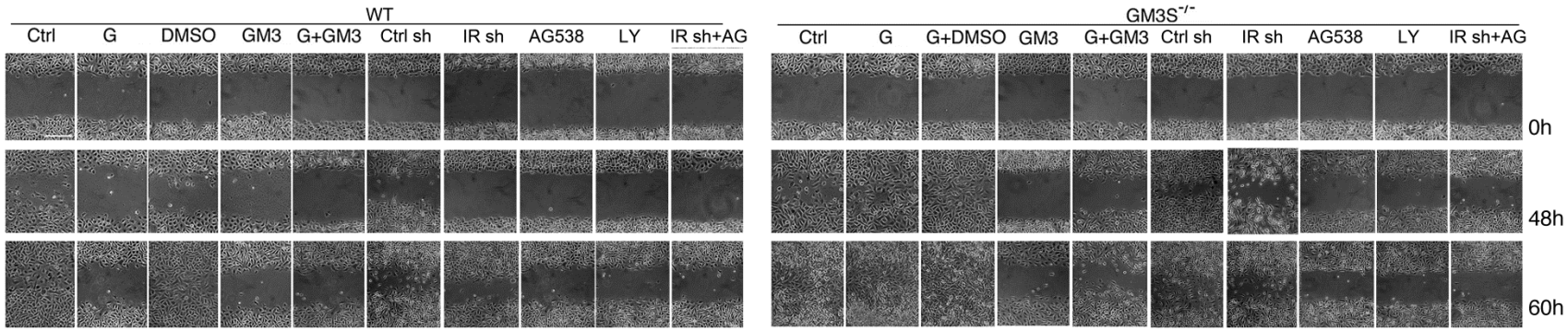

Supplemental Figure 6. **Accelerated migration of GM3S depletion requires IGF-1R activation**. Migration of mouse KCs in scratch assays were compared after treatment to increase glucose by 12 mM (G), increase GM3 (+50 μM), or suppress IR expression (transient transfection with IR shRNA-expressing lentivirus), IGF-1R activity (AG538/ AG), or PI3K (+20 μM LY294002; LY). Scratch assays depict the effect of representative biochemical and genetic interventions shown graphically in Fig. 5c, d, and e. Bar = 60 μM.

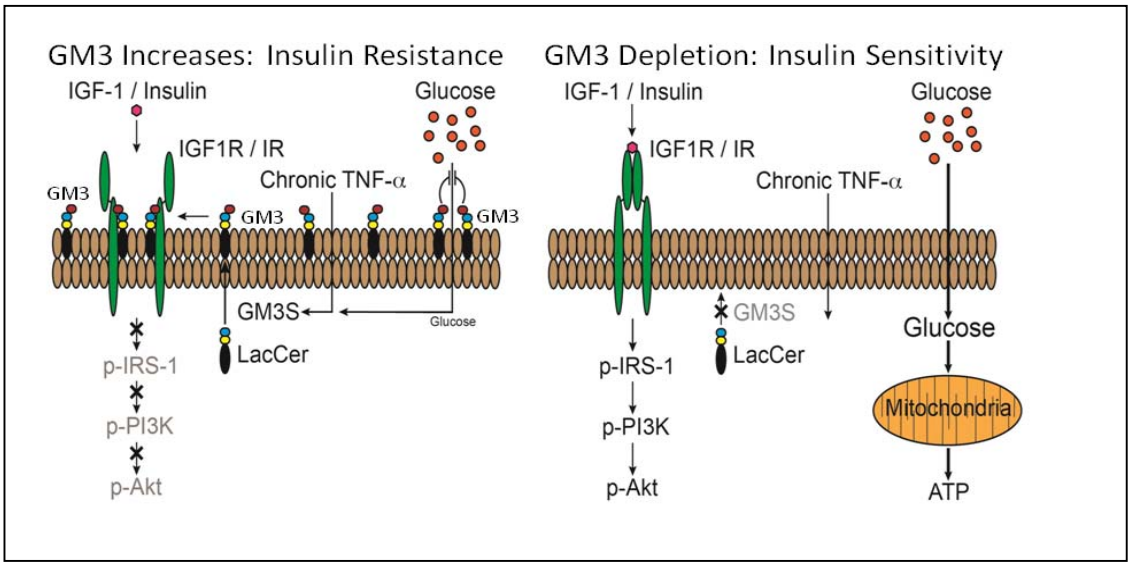

Supplemental Figure 7. **Proposed model of positive feedback loop of hyperglycemia and GM3 generation that perpetuates insulin resistance**. The increase in GM3, which suppresses IGF-1R and IR signaling, is prevented by GM3S depletion.